ANALYSIS OF DISPERSIVE WAVES BY WAVE-FIELD TRANSFORMATION

George A. McMechan and Mathew J. Yedlin

Abstract

The dispersive waves in a common-shot wave field can be transformed into images of the dispersion curves of each mode in the data. The procedure consists of two linear transformations: a slant stack of the data produces a wave field in the phase slowness-time intercept (p-τ) plane, in which phase velocities are separated; the spectral peak of the one-dimensional Fourier transform of the p-τ wave field then gives the frequency associated with each phase velocity. Thus, the data wave field is linearly transformed from the time-distance domain into the slowness-frequency (p-ω) domain, where dispersion curves are imaged. All the data are present throughout the transformations. Dispersion curves for the mode overtones as well as the fundamental are directly observed in the transformed wave field. In the p-ω domain, each mode is separated from the others even when its presence is not visually detectable in the untransformed data. The resolution achieved in the result is indicated in the p-ω wave field by the width and coherence of the image. The method is applied to both synthetic and real datasets.

Introduction

Surface-wave data are conventionally analyzed by treating small subsets (typically pairs of traces) of the observations (cf. Dziewonski and Hales, 1972). In this paper we develop an alternate approach to surface-wave analysis that consists of transforming the entire data wave field into the slowness-frequency (p-ω) domain where the dispersion curve can be directly picked. The process involves two linear transformations: a slant stack followed by a one-dimensional Fourier transform.

Examples of the processing of wave fields by slant stacking have been presented by McMechan and Ottolini (1980), Clayton and McMechan (1980), Phinney et al. (1980) and Stoffa et al. (1980). The result of this transformation is a wave field in the ray parameter-time intercept (p-τ) plane. The second transformation required is a one-dimensional Fourier transform over τ.

The wave-field transformation approach to data processing has the advantage that all the data contribute to the final image; there is no subjective selection of data (e.g. by picking of peaks and troughs or by frequency windowing) as is involved in conventional methods. In theory, since both the Fourier transform and slant stacking are reversible transformations, this approach could potentially be used to generate a synthetic surface-wave profile from characteristics of propagation specified in the p-ω plane. (This would require using the complex Fourier coefficients rather than just amplitudes as we do here for the inverse problem.)

In this paper we present the theory for the extraction of a dispersion curve from a common-shot wave field by a double transformation of the data. The method is illustrated with several synthetic examples and with two marine common-shot gathers.

Theory

The technique used to obtain the image of the dispersion curve from a wave field relies on the spectral decomposition of that wave field. To determine the transformation required to image the dispersion relation from the wave field, we begin with its frequency-wavenumber representation (Chapman, 1978),

$$V(x,t) = \int dk \int d\omega\, e^{i(kx-\omega t)} \frac{N(k,\omega)}{D(k,\omega)} \tag{1}$$

where x is offset, t is traveltime, k is wavenumber, N(k,ω) is a function of the source excitation, and D(k,ω) is the dispersion relation. Equation (1) is completely general, with no assumptions made about the nature of the wave field. Now, we apply a slant stack operator to both sides of (1) to get

$$U(p,\tau) = \int dx\; V(x,\tau+px) = \int dx \int dk \int d\omega\, e^{i[kx-\omega(\tau+px)]} \frac{N(k,\omega)}{D(k,\omega)} \tag{2}$$

Integration of the x integral yields $\delta(k-\omega p)$. Thus,

$$U(p,\tau) = \int dk \int d\omega\, e^{-i\omega\tau} \frac{N(k,\omega)}{D(k,\omega)}\, \delta(k-\omega p) \tag{3}$$

Equation (3) describes a transformation of the original wave field, and has a very

simple interpretation when the medium is horizontally stratified (Clayton and McMechan, 1980). Performing the wavenumber integration in (3), we obtain

$$U(p,\tau) = \int d\omega\, e^{-i\omega\tau} \frac{N(\omega p,\omega)}{D(\omega p,\omega)} \tag{4}$$

Finally, application of a Fourier transform over τ yields

$$U(p,\omega) = \frac{N(\omega p,\omega)}{D(\omega p,\omega)} \tag{5}$$

In the wave field $U(p,\omega)$ there will be a set of points that satisfies the dispersion relation $[D(\omega p,\omega)=0]$. On this locus, $U(p,\omega)$ becomes infinite. Thus, the p-ω locus corresponding to the largest values in the $U(p,\omega)$ wave field is exactly the dispersion curve that we seek.

Synthetic Examples

In order to investigate the performance of wave-field transformations applied to imaging dispersive waves, we processed a number of synthetic examples for which the results could be verified. One of these is shown in figures 1 and 2. Figure 1a contains a synthetic Love-wave profile computed for the single layer over a half-space model which is shown in figure 1b. Only the fundamental mode was included. The two transformations involved in imaging the dispersion relation are shown in figure 2.

Figure 2a contains the slant stack of the wave field in figure 1a. The p-τ wave field contains the same information as do the original data, but it is now decomposed into elements of equal phase velocity v (p=1/v). In the p-τ wave field (figure 2a), the dispersive nature of the data is clearly evident in the frequency content of the traces. The frequency becomes lower with decreasing p (increasing v). The slant stack introduces a phase distortion of the data (Chapman, 1978), but no frequency shift. Thus, the amplitude spectrum of the trace at a given p is identical to that associated with the corresponding phase velocity in the original data. The amplitude spectrum of each trace in figure 2a is plotted in figure 2b. The trajectory composed of spectral peaks should be the image of the dispersion curve for the model in figure 1b. For comparison, the correct dispersion curve is plotted in figure 2c.

A more complicated example is presented in figures 3 and 4. A synthetic Love-wave profile containing the fundamental and the first two higher modes was computed for the model in figure 1b. This wave field is shown in figure 3. The "shingling" of phase velocity loci oblique to the main (group velocity) trajectory, a characteristic of

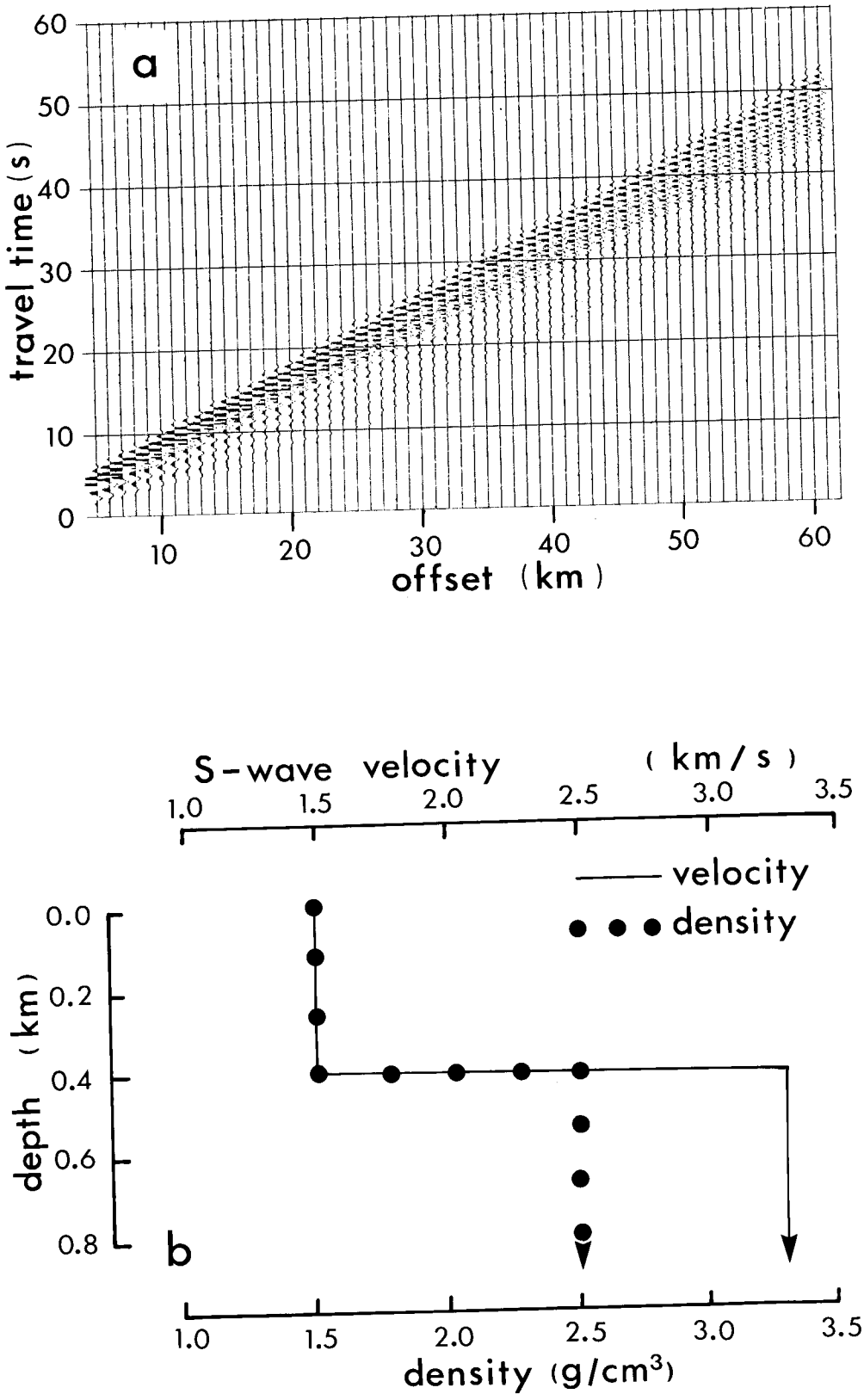

FIG. 1. Synthetic seismograms (a) for Love waves in a model consisting of a layer over a half-space (b). These seismograms contain only the fundamental mode. Dispersion can be seen clearly at the near offsets where the lowest frequencies arrive earliest. The extraction of the dispersion curve from these data is presented in figure 2.

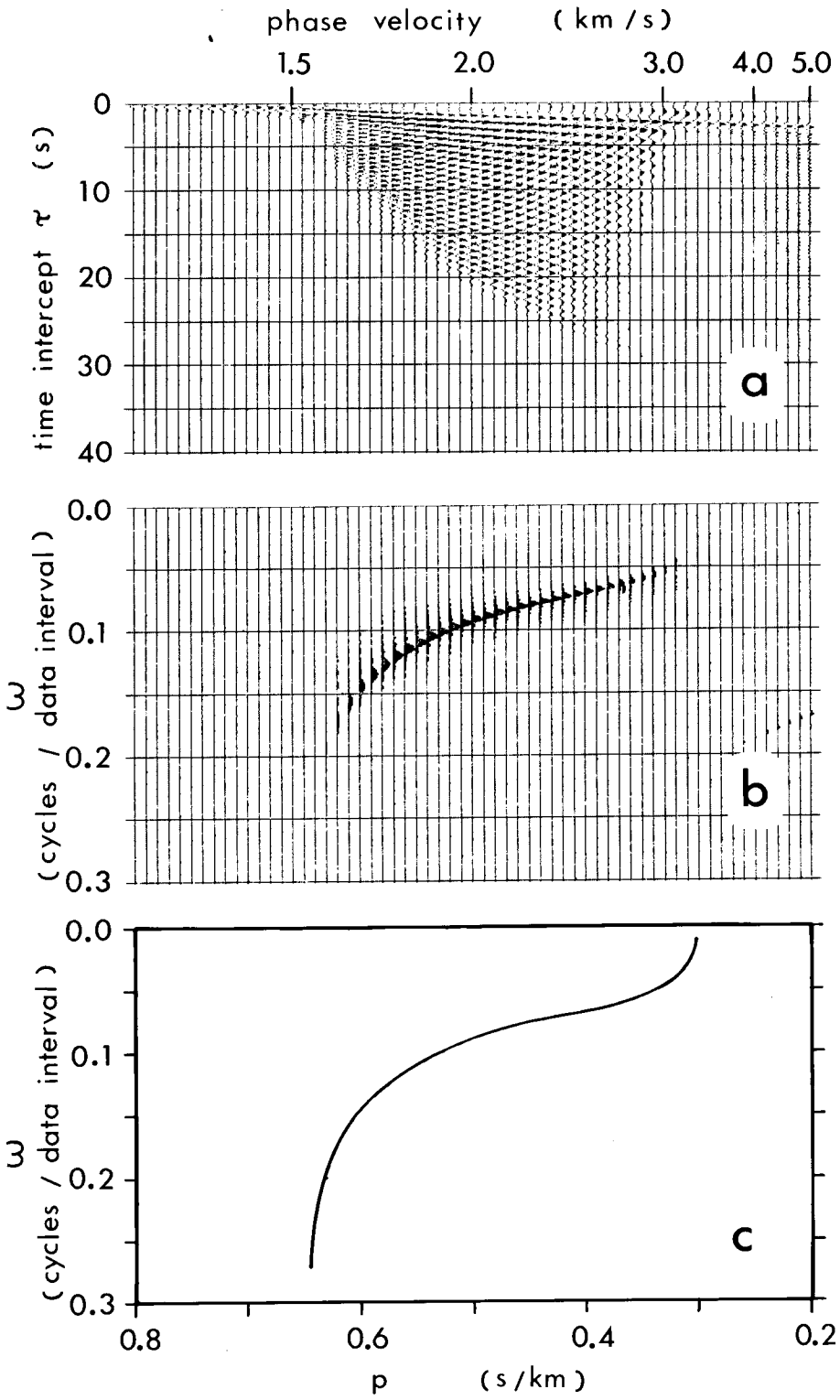

FIG. 2. The fundamental mode data in figure 1a were slant stacked to produce the p-τ wave field in (a). A one-dimensional Fourier transform (over τ) of the p-τ wave field produces an image in the p-ω domain (b) which corresponds to the dispersion curve. For comparison, the analytic dispersion curve is shown in (c). The data interval is 0.07s.

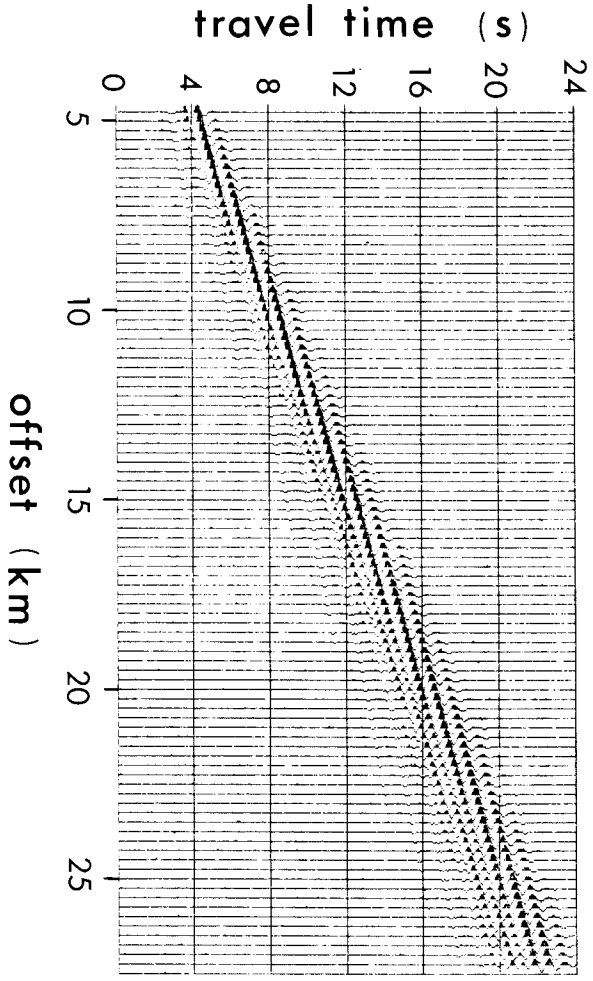

FIG. 3. Synthetic seismograms for Love waves in a model consisting of a layer over a half-space. These seismograms contain the fundamental mode and the first two overtones, although only the low frequency, high-amplitude fundamental is obvious. The procedure described in this paper can be used to detect all three modes and to find the dispersion curve of each. The results obtained by processing this seismogram profile are shown in figure 4.

dispersed wave trains, is clear in the data wave field. (The real data profiles in figure 5 also exhibit this effect.)

Figure 4a contains the p-ω transformation of the synthetic data profile in figure 3. In this wave field each of the three modes forms a separate, well-defined image. A comparison of the images with their expected positions, as given in figure 4b, indicates that they are correctly located. Some interesting features of the p-ω wave field (figure 4a) are the spectral holes labeled 1, 2 and 3. These holes are at the same frequency in each of the three dispersion curves. This is a source effect. The time source function used is

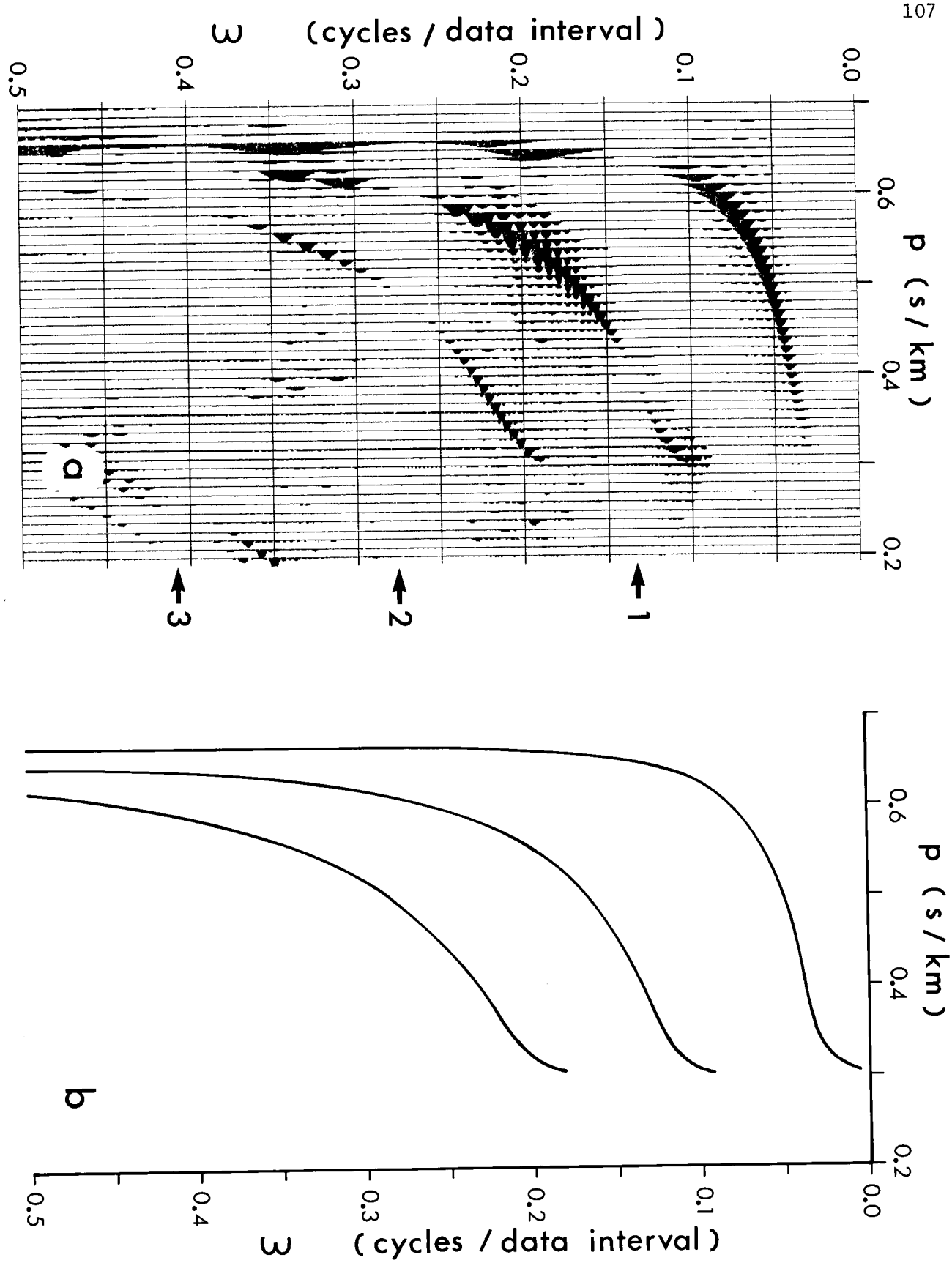

FIG. 4. Mode detection by wave-field transformation. The left (a) half of this figure shows the three images obtained by a Fourier transform of the slant stack of the seismograms in figure 3. Each image contains contributions from one entire mode in the data. The uppermost image is the fundamental mode; the lower two are the first two overtones. For comparison, the positions of the dispersion curves as determined analytically are shown in the left (b) half of the figure. The data interval is 0.04s.

a triangle, which has a $sinc^2(\omega)$ behavior in frequency. The spectral holes correspond to the zeros of the $sinc^2(\omega)$ function. Another way to think of this is that we are obtaining an image of N/D [equation (5)]. To find the image of D alone, the contribution of N must be deconvolved out.

The results obtained in the analysis of synthetic examples of dispersion, by double transformation of the data wave field, motivated a practical application. The processing of some real marine data is presented below.

Application to Marine Data

In this section we present two examples of the extraction of dispersion curves from recorded marine data. The two data profiles are shown in figure 5. The p-τ and p-ω transformations of the wave field in figure 5a are shown in figure 6, and those of the wave field in figure 5b are shown in figure 7. Both datasets produce coherent p-ω images. Because the data are recorded in a marine environment, we expect that the dispersed wave trains are Rayleigh-like waves. Note, however, that it is not necessary to make any assumptions about the wave type in order to extract the dispersion [see equation 5]. Each dispersed wave train present in a dataset will produce an image in the p-ω domain regardless of propagation characteristics, mode number, or whether its presence in the data is known *a priori* (see figure 4).

In figure 7c the dispersion curves obtained from both real datasets are shown. These curves are the loci of maximum spectral amplitude extracted from the p-ω wave fields in figures 6b and 7b. The uncertainty in these loci is indicated by the width and coherence of the p-ω images. An explicit estimate of uncertainty could be obtained by treating the spectral peak at each phase velocity as a probability density function. In the present case, it is clear that the two dispersion curves are separated; the phase velocities in the second dataset (the solid line in figure 7c) are consistently higher than those in the first (the dotted line).

Comments on Implementation

Although the basic concepts are straightforward, there are a number of practical points to consider in dispersion analysis by wave-field transformations. One particularly important one is that the sampling rates in both time and offset must be sufficiently high to avoid aliasing. In order to obtain an unaliased slant stack of a surface-wave train, the sampling rate in the offset coordinate must be greater than required for an

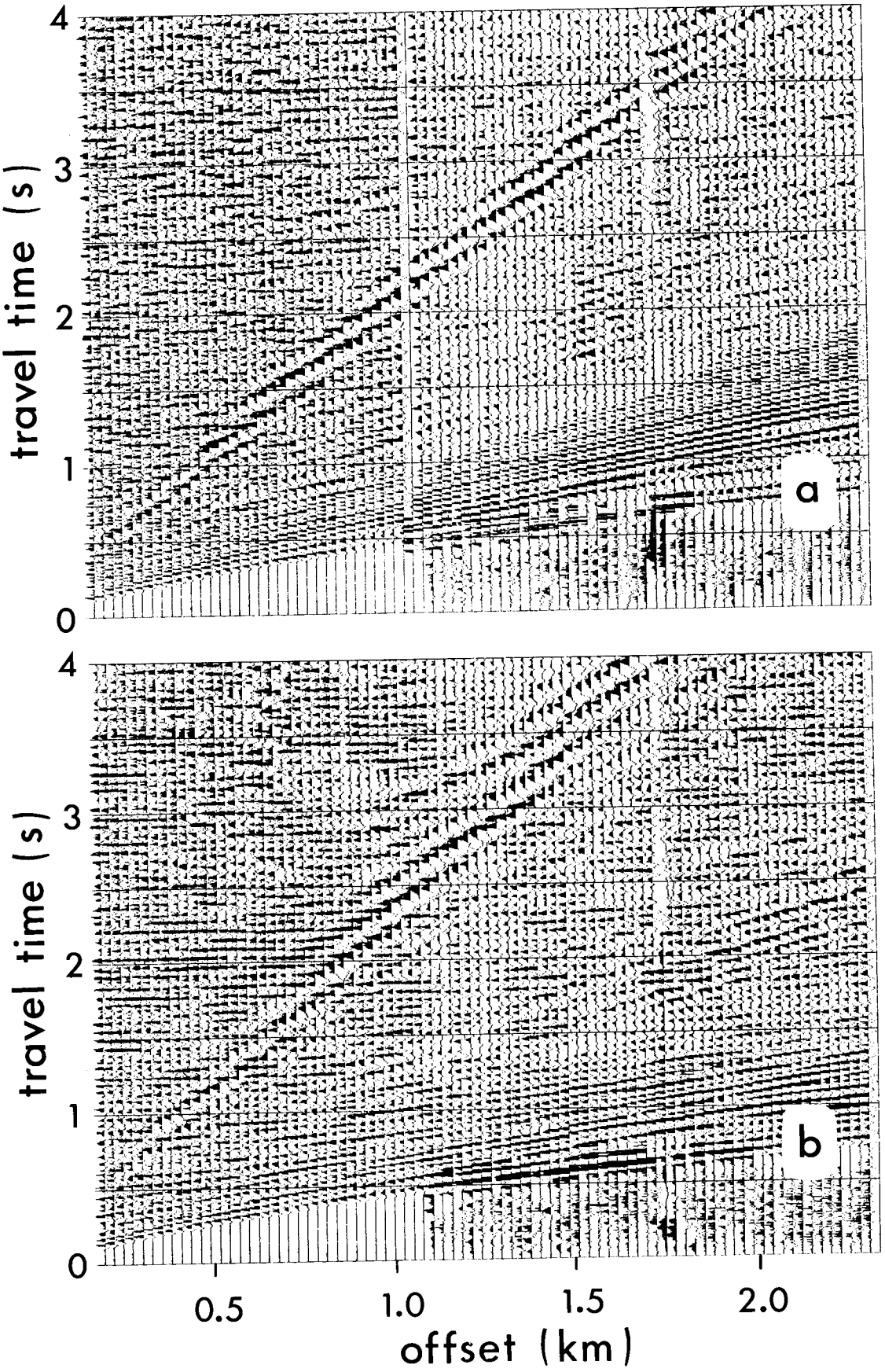

FIG. 5. Two marine profiles containing dispersive wave trains. The arrivals of interest are those that run from the lower left to the upper right. The earlier, high-frequency arrivals are body waves. The transformation of these two dispersed wave trains into the images of their dispersion curves is shown in figure 6 [for (a)] and figure 7 [for (b)].

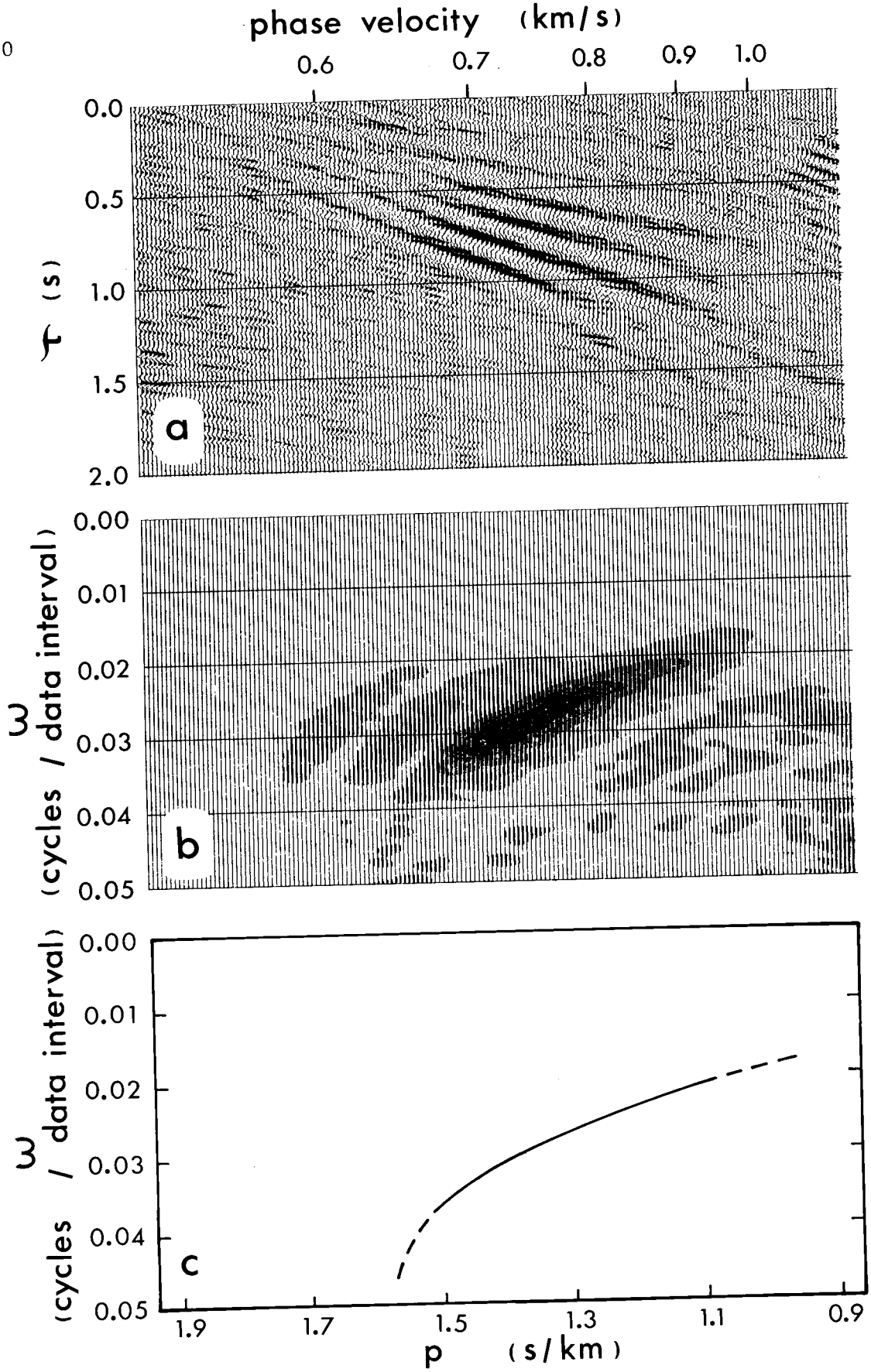

FIG. 6. The slant stack of the marine data profile in figure 5a is the p-τ wave field in (a). A Fourier transform of this wave field (over τ) produces the p-ω image in (b). The locus of maximum amplitude at each p in (b) is shown in (c) and is an estimate of the dispersion curve for the fundamental mode of the dispersed wave train in figure 5a. Higher modes were not found.

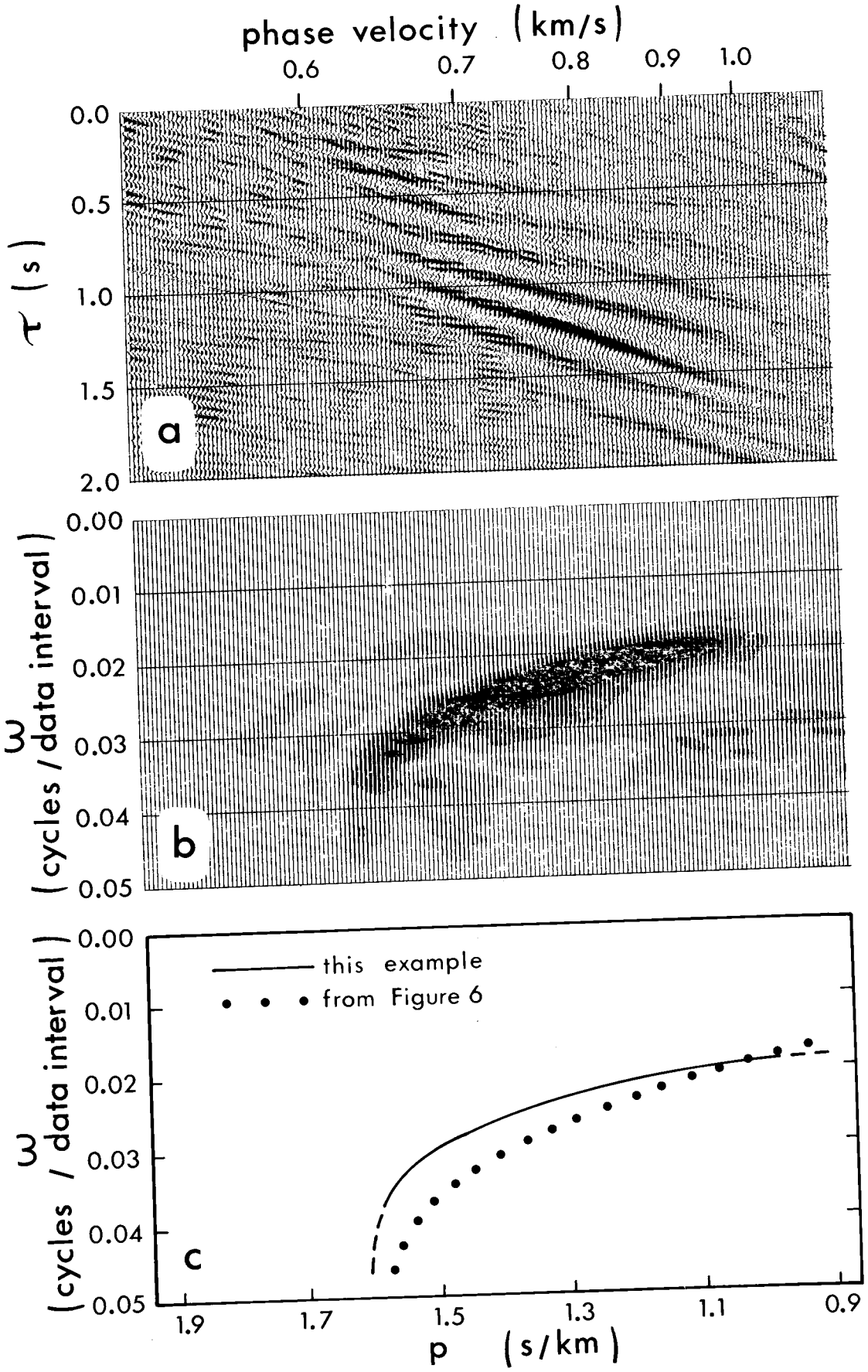

FIG. 7. Estimation of the dispersion curve of the dispersed wave train in figure 5b by double transformation of the entire data wave field. See caption of figure 6.

unaliased stack of the body waves in the same profile, because the velocity of surface waves is even less than that of the S-waves. Additional considerations in slant stacking are discussed by McMechan and Ottolini (1980).

The ω-extent of a p-ω image is restricted to the band-pass of the recording instruments combined with all other filtering procedures that have been applied to the data. Thus, it is desirable that the data be retained in as broadband a format as possible.

One obvious application of the results of this study is to provide an alternative to ω-k pie-slice filtering for the removal of dispersive waves from common-shot gathers. The shape of the required filter for any mode of any dispersed wave train is defined by the corresponding p-ω image. The filter can be applied in the p-ω domain. An inverse Fourier transform of the (complex) p-ω image followed by an inverse slant stack should produce a reconstructed time-offset profile with the dispersive waves removed.
Another possible extension is the migration of the p-ω image to produce a velocity-depth profile directly via the application of the results of Takahashi (1955), as suggested by Clayton and McMechan (1980). These applications are currently being investigated

Conclusions

In this paper we have demonstrated a wave-field transformation method for analysis of dispersed wave trains. The process consists of two linear transformations. A slant stack decomposes the data wave field into elements of constant phase velocity. The frequency associated with each phase velocity is then obtained by a one-dimensional Fourier transform. The main advantages of the method are that the entire wave field is present throughout both transformations and that the desired feature (the dispersion curve) is extracted directly from its image in the transformed wave field. The method has been used to analyze a pair of common-shot marine profiles.

ACKNOWLEDGMENTS

During the course of this project one of the authors (G.M.) was on leave at the Stanford Exploration Project, Department of Geophysics, Stanford University, which provided superb computing facilities. Critical reviews of the paper by R. Stolt and R. Clayton were much appreciated. The real data gathers were kindly provided by O. Yilmaz of Western Geophysical Company. The computer code used to generate the synthetic examples was provided by D. Boore of the U.S. Geological Survey, Menlo Park. Both Western Geophysical and the U.S.G.S. are sponsors of the Stanford Exploration Project. The authors benefited from discussions with R. Clayton, P. Spudich, D. Boore and R. Stolt. The work was supported in part by the Department of Energy, Mines & Resources, Canada.

REFERENCES

Chapman, C.H., 1978, A new method for computing synthetic seismograms: Geophys. J., v. 54, p. 481-518.

Clayton, R.W., and McMechan, G.A., 1980. Inversion of refraction data by wave-field migration: Geophysics, submitted.

Dziewonski, A.M., and Hales, A.L., 1972, Numerical analysis of dispersed waves, in Methods in Computational Physics, v. 11, p. 39-85, New York, Academic Press.

McMechan, G.A., and Ottolini, R., 1980, Direct observation of a p-τ curve in a slant stacked wavefield: SSA Bull., in press.

Phinney, R.A., Chowdhury, K.R., and Frazer, L.N., 1980, Transformation and analysis of record sections: preprint.

Stoffa, P.L., Buhl, P., Diebold, J.B., and Wenzel, F., 1980, Direct mapping of seismic data to the domain of intercept time and ray parameter; A plane wave decomposition: preprint.

Takahashi, T., 1955, Analysis of dispersion curves of Love waves: Bull. Earthq. Res. Inst., v. 33, p. 287-296.